EFFECTS OF OSMOTIC AGENT CONCENTRATION AND TYPE ON THE PERFORMANCE OF OSMOTIC MEMBRANE DISTILLATION

Qusay Fadhel Alsalhy[1], Najat Jumaa Saleh, Nisreen Sabah Ali
Chemical Engineering Department, Oil and Gas Refinery Engineering, University of Technology,
Baghdad, Iraq
qusayalsalhy@yahoo.com; qusayalsalhy@uotechnology.edu.iq

ABSTRACT

A thin Polytetrafluoroethylene (PTFE) microporous layer supported by a polypropylene (PP) net (TF200 from pall–Gelman) with 0.00275 m² total surface area of the membrane was used for the removal of water from dilute aqueous solutions in osmotic membrane distillation process. The influence of osmotic agent concentration and type such as, (1–5 mol/L) calcium chloride (CaCl$_2$) and (2–5 mol/L) sodium chloride (NaCl) on the transmembrane flux was studied. The increase in the osmotic agent concentration (both of calcium chloride and sodium chloride) resulted in an increase in transmembrane flux. The calcium chloride (CaCl$_2$) showed higher transmembrane flux as compared to sodium chloride (NaCl). Besides, it was found that, there is no transmembrane flux using 1 mol/L of sodium chloride NaCl solution. Empirical correlation comprising of dimensionless numbers was used in order to estimate the water transport through the boundary layers (feed as well as osmotic agent OA side). The mass transport of water through the membrane has been estimated based on mode of diffusion mechanism in the pores by Knudsen or molecular diffusion. Theoretical results were estimated and compared with the experimental results. Based on the experimental results of OMD process, it was found that, there are 17% deviations between the

theoretical and experimental results.

INTRODUCTION

Osmotic membrane distillation (OMD) is one of the membrane distillation (MD) variants, operated at low temperature. The MD comprises a relatively novel membrane process, which can be applied for the separation of various aqueous solutions. The hydrophobic membranes, with the pores filled by the gas phase, are used in this process [1,2]. The advantages of osmotic membrane distillation compared to other separation processes can be summarized as: ambient operating temperature and pressure; less demanding mechanical membrane properties required; no or less degradation of heat-sensitive components; and higher concentrated feed can be achieved. OMD is a membrane transport process in which a liquid phase (most commonly an aqueous solution) containing one or more volatile components is allowed to contact one surface of a micro-porous membrane whose pores are not wetted by the liquid, while the opposing surface is in contact with a second non-wetting liquid phase in which the volatile components are soluble or miscible. The membrane thereby functions as a vapor gap between the two liquid phases, across which any volatile component is free to migrate by either convection or diffusion. The driving potential for such transport is the difference in vapor pressure of each

component over each of the contacting liquid phases [3].

Mansouri and Fane (1999) [4] described the development of modified hydrophobic membranes for osmotic distillation (OD) which are tolerant to oily feeds. Three commercial membranes were chosen as substrates including the Celgard 2500, Millipore GVSP and the UPVP (UHMWPE, Millipore). The focus has been on using PVA coatings which were found to have an insignificant effect on flux. Several models commonly employed to represent the mass transfer in osmotic distillation (OD) systems are applied by Courel et al, to the results of pure water OD experiments carried out with two commercial asymmetric porous membranes. Besides, Molecular and Knudsen diffusion mechanisms are tested to model the vapour transport across the membrane [5]. Also Courel et al., (2000b) [6] studied a recent membrane technique osmotic distillation (OD), which is used to concentrate binary water–sucrose solutions at ambient temperature under atmospheric pressure. Naveen et al., (2006) [7], studied the effect of various process parameters such as, concentration and flow rate of the osmotic agent; type of (polypropylene membranes) and pore size (0.05 and 0.2 μm) of the membrane; temperature with respect to transmembrane flux. Experiments were performed with real systems (pineapple/sweet lime juice) in a flat membrane module. Osmotic agents namely sodium chloride and calcium chloride at varying concentrations are employed. For both the osmotic agents, higher transmembrane flux was observed at maximum osmotic agent concentration. A mass transfer-in-series resistance model has been employed, considering the resistance offered by the membrane as well as the boundary layers (feed and brine sides) in case of real systems for the first time. The model could predict the variation of transmembrane flux with respect to different process parameters. Ravindra Babu et al., (2006) [8]

evaluated the effect of various process parameters, such as concentration and flow rate of feed and osmotic agent on the transmembrane flux in case of phycocyanin and sweet-lime juice. Mesoporous (pore size 0.05μm) and macroporous (pore size 0.2μm) hydrophobic polypropylene membranes were used in the study. The increase in the osmotic agent concentration and flow rate resulted in an increase in transmembrane flux. The feed and osmotic agent side mass transfer resistances were estimated based on classical empirical correlation of dimensionless numbers, whereas membrane resistance was estimated using Dusty-gas model. The mass transfer mechanism was found to be in the transition region that is between Knudsen and molecular diffusion [8]. Thanedgunbaworn et al., (2007) [9] carried out the osmotic distillation process on a polyvinylidenefluoride (PVDF) hollow fiber membrane module using fructose solutions and clarified grape juice as feeds. The main characteristics of the fibers are 0.66 mm internal diameter, 170 μm thickness, 0.2 μm pore diameter and 64% porosity. The influence of operating parameters such as feed and brine flow velocities, feed concentration, and temperature, on the osmotic distillation flux was studied. Temperature and feed concentration had significant effect on flux. On the contrary, the increase of feed and brine velocity or the hydrodynamic conditions can cause the OD flux enhancement.

The objective of the present work is to study the effect of osmotic agent concentration and type on performance of Polytetrafluoroethylene (PTFE) membrane supported by a polypropylene (PP) net (TF200 from pall–Gelman) used in osmotic membrane distillation process. Knudsen and molecular diffusion mechanisms are used for modeling the vapour transport through the membrane. Classical correlation of dimensionless numbers is used to predict the boundary layer mass

transfer coefficient within the feed and osmotic agent side. It is worth noting that a systematic study of the effect of the temperature difference (because of latent heat of vaporization and condensation across the membrane wall) on the transmembrane flux has not been reported extensively. Therefore, the thermal effects associated with mass transfer in OD are estimated in this work.

THEORY

Eq. (1) is used to describe the transport of water in the system that relates the mass flux (J) to the vapor pressure difference across the membrane (ΔP), via a proportionality coefficient (K) which is considered as membrane permeability:

$$J = K \ \Delta P \qquad (1)$$

The vapor pressure difference depends on the osmotic agent concentration and the temperature prevailing across the membrane. Eq. (2) represents the overall mass transfer coefficient for all the three resistances for water transport:

$$K = \left[\frac{1}{K_f} + \frac{1}{K_m} + \frac{1}{K_p} \right]^{-1} \qquad (2)$$

Where $(\frac{1}{K_f})$, $(\frac{1}{K_m})$, and $(\frac{1}{K_p})$ are the mass transfer resistance in feed solution, composite membrane and osmotic agent layer respectively, (see Fig. (1)).
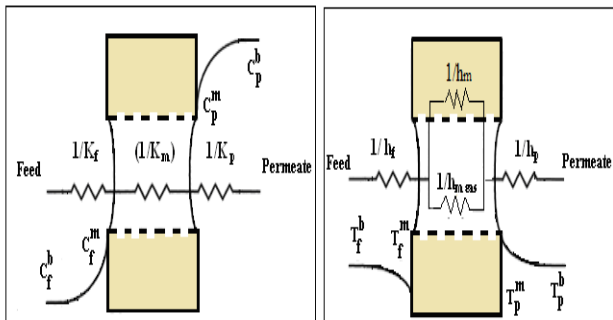

(a)   (b)
Fig.1. (a) Concentration profile and mass transfer resistances in osmotic distillation, (b) Temperature profile and heat transfer resistances in osmotic distillation

The vapor transfer mechanism through the membrane mainly depends on structure of the membrane and partial pressures across the membrane. There are two mechanisms can be theoretically involved in the vapor transfer: Molecular diffusion and Knudsen diffusion and the corresponding membrane permeability can be expressed by Eqs. (3) and (4), respectively [10]:

$$K_m^M = \frac{M_w D_{wa} \varepsilon P}{RT \delta \chi (P_a)_{Lm}} \qquad (3)$$

$$K_m^K = \frac{0.334 M_w \varepsilon d}{RT \delta \chi} \sqrt{\frac{8RT}{\pi M_w}} \qquad (4)$$

Two important factors affecting mass transfer through the membrane are the mean molecular free path of the vapor molecule transferred λ (m), and the mean pore diameter of the membrane d (m). The Knudsen number (K_n) can be defined as a physical quantity and expressed by Eq. (5):

$$K_n = \lambda / d \qquad (5)$$

Where $\lambda = \frac{k_B T}{1.4 P \pi \sigma^2}$

λ is expressed as a function of temperature (T), pressure (P) and mean collision diameter of the molecule (σ) depending on the gas kinetic theory. For a relatively small pore size, $K_n \geq 1$, the diffusing molecules tend to collide frequently with the pore walls, and Knudsen diffusion is the prevailing mechanism. When the pore size is relatively large, $K_n \leq 0.01$, the collisions between the gas molecules themselves are more frequent and molecular diffusion is considered predominant. Between these two limits, both mechanisms will coexist. The combination of different gas transfer mechanisms can be described by the Dusty gas model which is a general approach accounting for

mass transport in porous media [11].

The liquid mass transfer coefficients depend on the properties of the solutions and on hydrodynamic conditions of the systems. With the help of empirical correlation, these coefficients can be calculated. The water diffusion coefficient can be estimated by using the following empirical Eq. [12,13].

$$D_w = \frac{1.17 \times 10^{-16} T \sqrt{M_w \varphi}}{\mu \nu_A^{0.6}} \tag{6}$$

The liquid mass transfer coefficients in the boundary layers of feed and osmotic agent (permeate) (k_f and k_p) can be estimated by using empirical equations given below [14]:

$$Sh = b_1 \, Re^{b2} \, Sc^{b3} \tag{7}$$

where, b_1, b_2 and b_3 are the constants and are to be selected appropriately for the given hydrodynamic conditions, and

$$Sh = \frac{d_a k_i}{D_w}, Re_M = \frac{\rho N_A d_a^2}{\mu} \text{ and } Sc = \frac{\mu}{\rho D_w} \tag{8}$$

Where D_w is the water diffusion coefficient and can be estimated by using Eq. (6), d_a is the diameter of agitator, N_A rotational speed of agitator, ρ the density and μ the dynamic viscosity of the fluid.

In order to obtain K_f and K_p in the same units of K_m the following equation can be used [5]:

$$K_j = \frac{k_j C^t M_w}{P^* (x_s)_{Lm} \gamma} \tag{9}$$

where C^t is the molar concentration of the solution, γ activity coefficient and P^* the saturation vapor pressure, the values of which were obtained from literature [15-17].

The process of OD is usually isothermal as long as no external temperature difference is imposed across the membrane. However, at the present operating temperature (i.e., 30 ºC), evaporation at the membrane wall occurs, due to the absorbance of the latent heat from the feed, therefore the feed side

of the membrane became a bit cool. On the other hand condensation occurs on the other side of the membrane due to the loss of the latent heat, hence a slight temperature rise at the brine side. As a result, a mass transfer is established associated with heat transfer. Besides, the resulting temperature difference translates into a lower vapor pressure gradient lead to driving force decay. The latent heat for phase changes has to be transported between the bulks of the solution and the vaporization or condensation interfaces [5]. Fig.1b depicts the heat transfer mechanism in OD as a set of resistances with the temperature profile for the particular case of imposed mean bulk temperature. As established for MD [1], the balance of heat transfer in the various compartments of the system is given by equation (10) and the overall heat transfer coefficient of the OD process is given by Eq. (11):

$$Q = H\Delta T^b = h_f\left(T_f^b - T_f^m\right) = J\Delta H_v + h_m\left(T_f^m - T_p^m\right) = h_p\left(T_p^m - T_p^b\right) \tag{10}$$

$$H = \left(\frac{1}{h_f} + \left[1 \middle/ \left(h_m + \frac{J\Delta H_v}{\Delta T_m} \right) \right] + \frac{1}{h_p} \right)^{-1} \tag{11}$$

where Q is the total heat transferred across the membrane, J the molar vapor flux and ΔH_v the mass latent heat of vaporization; h_f and h_p represent the heat transfer coefficients of the feed and permeate boundary layers, respectively and h_m is the heat transfer coefficient of the membrane.

The transmembrane temperature difference ΔT_m for liquids in both sides is given by the following equation:

$$\Delta T_m = -J\Delta H_v \left[h_m + \left(\frac{1}{h_f} + \frac{1}{h_p} \right)^{-1} \right]^{-1} \qquad (12)$$

The thermal balance of the OD system helps highlighting the fundamental difference with the MD process. In the case of OD, the latent heat of vaporization $J\,\Delta H_v$ is integrally compensated by conduction across the composite membrane, $h_m\,\Delta T_m$. This conductive back heat flux occurred across the composite membrane, because of the temperature difference between the two sides of the composite membrane due to the absorbance of the latent heat from the feed and loss it on the permeate side.

Therefore, OD membranes will have to be as heat conductive as possible. In an MD process, the conduction of heat across the membrane is a loss mechanism since it has no corresponding transfer of mass and should thus be minimized [18]. The conduction heat transfer coefficient of the membrane is given by Eq. (13) where the total thermal conductivity k^T is a combination of the thermal conductivity of the gases — a mixture of air and water vapor — and of the membrane polymer [19]:

$$h_m = k^T \Big/ \delta \qquad (13)$$

$$K^T = \varepsilon\, k_{Gas}^T + (1-\varepsilon) k_{poly}^T \qquad (14)$$

The water vapor pressures within the membrane are not directly measurable, and then it is convenient to express Eq. (15) in terms of temperature. For low values of the transmembrane bulk temperature difference $(T_{b,f} - T_{b,p}) \leq 10\,°K)$, the following expression may be used as indicated in (Wilke and Chang, 1955) [12].

$$J = K_m \left(\frac{dp}{dt} \right)\!\left(T_{m,f} - T_{m,p} \right) \qquad (15)$$

where $\left(\dfrac{dp}{dt} \right)$ can be evaluated from the Clausius Clapeyron equation, using Antoine equation to calculate the vapor pressure [5,21].

$$\left(\frac{dp}{dT} \right)\! T_m = \frac{\Delta H_v}{RT_m^2}\, e^{\left(23.24 - \frac{3842}{T_m-45} \right)} \qquad (16)$$

The liquid heat transfer coefficients depend on the physical properties of the solutions and on the hydrodynamic conditions prevailing in the module. Therefore, h_f and h_p can be estimated either from experiments or with the help of empirical correlations of dimensionless numbers, such as Nusselt (Nu), Reynolds (Re) and Prandtl (Pr) numbers. The example given by correlation (17) corresponds to the heat transfer coefficient hl for a liquid flow in a tube.

$$Nu = 0.027\,Re^{4/5}\,Pr^{0.3} \qquad (17)$$

where $\qquad Nu = \dfrac{hl\,dh}{k^T}$ and $Pr = \dfrac{\mu cp}{k^T}$

The physical properties of the feed and osmotic agent OA solutions were evaluated from literature [14].

Experimental

The set-up used to conduct the osmotic membrane distillation (OMD) experiments is shown schematically in Fig. 2. The central part of the system is consisted of two identical stainless steel (SS-316) cylindrical chambers (60mm inside diameter and 95mm in length). One of the chambers is connected to a heating system through its jacket to control the temperature of the distilled water. The other chamber is connected to another heating system to control the osmotic agent temperature. The membrane was placed between the two chambers (distilled water side and permeate side). Osmotic agent solution chamber filled with salt solution of NaCl and CaCl$_2$ separately. The distilled water and osmotic agent temperatures were maintained at a temperature of 30 ºC throughout the

entire experiments. The temperatures were measured inside each chamber by a pair of sensors connected to a digital meter with an accuracy of ±0.2 ºC.

Flat-sheet commercial membrane, TF200 from pall–Gelman was used in this study. It was made of a thin Polytetrafluoroethylene (PTFE) macroporous layer supported by a polypropylene (PP) net.
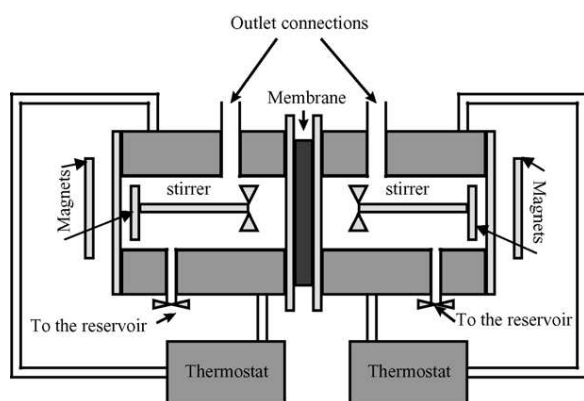

Fig. 2. Schematic diagram of the experimental apparatus

The total surface area of the membrane was of 2.75×10^{-3} m² and all membrane characteristics are listed in Table 1. The distilled water was brought into contact with the PTFE top layer of the membrane and permeate is in contact with the polypropylene (PP) of the membrane. Both liquids were stirred inside the chambers by magnetic stirrers with 42 rpm stirring rate. The CaCl2 solution is prepared from 1; 2; 3; 4; and 5mol/L CaCl2, while the NaCl solution is prepared from 2; 3; 4; and 5 mol/L NaCl. The transmembrane flux was calculated by measuring the increase in volume of osmotic agent every 30 minutes. All the experiments were performed for a period of 3 h and the average values of the flux with the standard deviation were reported. The concentrations of CaCl2 and NaCl solutions of both permeate and feed were measured by a Metrohm Ω 712 Digital conductivity meter types 1.712.0010.

Table1. Characteristics of the pall–Gelman Polytetrafluoroethylene (PTFE) microporous layer supported by a polypropylene (PP) net

Membrane area (m²)	2.75×10^{-3}
Membrane thickness (µm)	55 ± 6
Liquid entry pressure of water LEP_w (bar)	2.76 ± 0.09
Void volume ε (%)	69 ± 5
Mean pore size d_P (nm)	198.96
Effective porosity ε / L_P (m^{-1})	7878.1
Measured total composite membrane thickness δ (µm)	165 ± 8

Results and discussion

The value of the transmembrane flux was obtained by adjusting the experimental data (i.e., volume collected into the permeate side versus time) to a linear relation. As an example of the calculations carried out, the values of the slopes was estimated with their estimated standard deviations, in the case of solution concentration was varied between the values 1; 2; 3; 4; and 5 mol/L CaCl2 and 2; 3; 4; 5 mol/L NaCl with 42 rpm stirring rate and temperature 30°C. Tables 2 and 3 show effect of calcium chloride ($CaCl_2$) and sodium chloride (NaCl) concentration as osmotic agent on transmembrane flux. It can be seen that, with an increase of osmotic agent concentration in both calcium chloride ($CaCl_2$) and sodium chloride (NaCl), the transmembrane flux increased. This is due to the increase in vapor pressure difference across the membrane with an increase in the concentration of osmotic agent solution, which resulted in an increase in the driving force for water transport through the membrane [8]. Regarding the effect of type of osmotic agent on transmembrane flux, calcium chloride ($CaCl_2$) showed higher transmembrane flux than sodium chloride (NaCl) as shown in Tables 2 and 3, and Fig. 3.
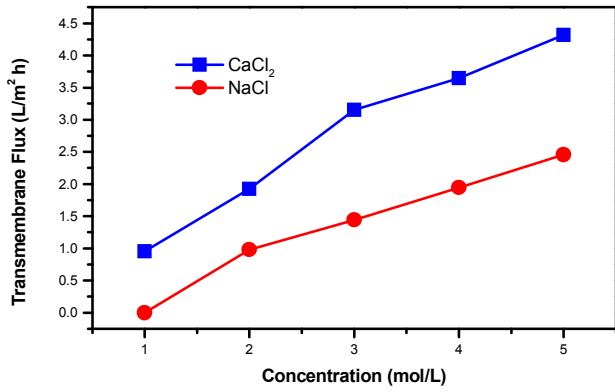
Fig. 3 Effect of osmotic agent concentration on the
transmembrane flux at 3 hr

Table 2. Effect of $CaCl_2$ concentration on the membrane permeate flux

Molarities of $CaCl_2$ (mol/L)	Flux $(L/m^2.h)$						
	0 (hr)	0.5 (hr)	1 (hr)	1.5 (hr)	2 (hr)	2.5 (hr)	3 (hr)
1	0.998±2.08E-05	0.986±7.79E-06	0.982±8.87E-06	0.961±2.50E-05	0.961±1.67E-05	0.961±1.47E-05	0.954±1.26E-05
2	1.934±6,11E-05	1.920±8.29E-05	1.846±4.95E-05	1.969±7.87E-05	1.725±22.9 E-05	1.883±5.53E-05	1.923±6.531E-05
3	3.249±9.49E-05	3.218±6.05E-05	3.291±4.93E-05	3.198±7.09E-05	3.075±16 E-05	2.971±6.85E-05	3.153±7.08E-05
4	4.283±5.97E-05	4.248±9.09E-05	4.025±14.2E-05	3.969±17.3E-05	4.184±4.69E-05	3.520±11.6E-05	3.643±23.31E-05
5	5.197±19.8E-05	5.066±6.99E-05	5.025±8.25E-05	4.840±6.88E-05	4.641±12.9E-05	4.428±14.1E-05	4.316±9.66E-05

Table 3. Effect of NaCl concentration on the membrane permeate flux

Molarities of NaCl (mol/L)	Flux $(L/m^2.h)$						
	0 (hr)	0.5 (hr)	1 (hr)	1.5 (hr)	2 (hr)	2.5 (hr)	3 (hr)
1	0	0	0	0	0	0	0
2	1.022±2.43E-05	1.147±4.00E-05	1.173±4.40E-05	1.138±4.27E-05	1.276±20.0E-05	1.184±21.7E-05	0.978±2.965E-05
3	1.522±4.59E-05	1.471±2.91E-05	1.452±22.5E-05	1.457±4.56E-05	1.423±1.55E-05	1.453±6.61E-05	1.442±1.28E-05
4	2.186±4.47E-05	2.022±10.2E-05	2.000±4.65E-05	1.989±5.64E-05	1.975±5.08E-05	1.898±1.64E-05	1.946±1.58E-05
5	3.178±59.4E-05	2.661±10.3E-05	2.694±9.36E-05	2.710±8.62E-05	2.363±14.3E-05	2.440±9.22E-05	2.456±15.22E-05

This is mainly due to the higher osmotic activity (ratio of its water solubility to its equivalent weight) of CaCl2·2H2O, which has resulted in higher vapor pressure gradient across the membrane and thus lead to increased the transmembrane flux. Nagaraj et al. (2006)[7] reported that, the calcium chloride (CaCl2) has showed higher transmembrane flux at all the concentrations when compared to that of sodium chloride (NaCl), because of higher osmotic activity of the calcium chloride than that of sodium chloride.

Tables 2 and 3, show the effect of $CaCl_2$ and NaCl concentration on the transmembrane flux as a function of time. It can be seen that, with an increase of the concentration of the osmotic agent in both cases as a function of time, the transmembrane flux decreased and the best transmembrane flux is found at the first minutes of the experiment. For example, using $CaCl_2$ (i.e., 5 mol/L) as osmotic agent the transmembrane flux decrease from 5.1972 at zero hour to 4.31659 (L/m2.h) at 3 hour, and using NaCl (i.e., 5 mol/L) the transmembrane flux decrease from 3.1786 to 2.456 (L/m2.h) as shown also in Tables 2 and 3. This is attributed to the membrane fouling occurring in the first few minutes of the experiment. It means that, the concentration of CaCl2 and NaCl solutions is an important factor strongly affecting the speed of membrane fouling [22,23]. Moreover, with time, the osmotic agent solution becomes progressively more diluted, especially at higher concentrations of the osmotic agent solution that lead to higher transmembrane fluxes. When the osmotic agent solution is diluted, the driving force available is also reduced and, therefore, there is a decay of flux.

To compare the theoretical and experimental results in both cases, theoretical fluxes were estimated by accounting the individual mass transfer coefficient for boundary layers (feed and osmotic agent OA) as well as for membrane as shown in Table 4. In order to estimate the water transport through the boundary layers (feed as well as osmotic agent OA side), empirical correlation comprising of dimensionless numbers (Eq. (7)) was used and the membrane module employed is flat.

Table 4. Values of mass transfer coefficient at different concentrations of osmotic agent

Concentration (M)	K_p ($\times 10^4$ m s^{-1})
a. For $CaCl_2$	
1	2.501959
2	3.092461
3	3.936354
4	5.476957
5	8.627225
b. For NaCl	
2	5.425339
3	5.371074
4	5.220535
5	5.028386

k_m = 1.196276E-02 kg m^{-2} h^{-1} Pa^{-1}.

k_f = 4.834239 $\times 10^{-5}$ m s^{-1}

The values of the constants in Eq. (7) are considered as b_1 = 0.027, b_2= 4/5 and b_3= 0.4 [12]. Mass transport of water through membrane has been estimated based on mode of diffusion mechanism in the pores by Knudsen or molecular diffusion (Eq. (3) or (4)). It may also be noted that the mechanism of mass transfer in the membrane could not be clearly pointed out to be either Knudsen or molecular [14,23,24]. This may be mainly due to the fact that the membranes employed by those researchers are composite type, where mechanism will be different in the active layer compared to the support layer. In the present work, it has been found that $K_n \leq 0.01$, taken into account the effect of temperature difference on either sides as explained in the theoretical section, hence the molecular diffusion is predominate.

The heat transfer coefficients of the boundary layers (feed and osmotic agent OA) were estimate

from empirical correlation of dimensionless numbers (Eq. (17)), and the membrane heat transfer coefficient was estimated using Eq. (13) where the total thermal conductivity was estimate from Eq. (14), the thermal conductivity of the gases k_{Gas}^{T} = 0.027 W/m.K and the thermal conductivity of the membrane polymer k_{poly}^{T} = 0.22 W/m.K (for PTFE and PP support layers) [21, 25]. Theoretical values of the transmembrane flux could be estimated after calculating the overall mass transfer resistance (membrane and boundary layers) and water vapor pressure within the membrane. Simulation is done with the aid of a FORTRAN computer program.

Figs. 4 and 5 represent the comparison between experimental and theoretical transmembrane fluxes for calcium chloride CaCl2 and sodium chloride NaCl, respectively. It can be seen that, there are 17% deviations between the theoretical and experimental results. This deviation attributed to the heterogeneous structure and pore size distribution of the poly (tetrafluoroethylene) (PTFE) microporous layer supported by a (PP) net (TF200) membrane. Besides, the thin PTFE layer has high ability for water transport in vapour phase, while the polypropylene supported layer contributes to the mass transfer resistance in the liquid form.
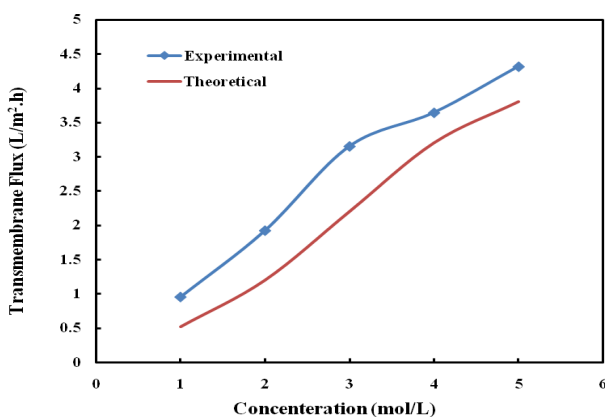

Fig. 4 Comparison between theoretical and experimental transmembrane flux for CaCl$_2$ solution
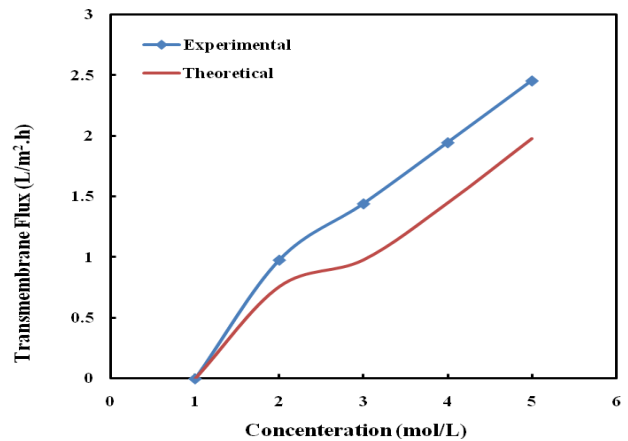

Fig. 5 Comparison between theoretical and experimental trans-membrane flux for NaCl solution

Nagaraj et al. (2006) [7], reported that the observed deviations of the predicted values from the experimental values of the transmembrane flux could be attributed to uneven pore distribution, geometry of the membrane and complex hydrodynamic nature of the boundary layer (feed and osmotic agent). On the other hand, the deviation between the theoretical and experimental results in the present work was 1.5 fold lower than that discussed in the literature [8,24]. Because of the thermal effect due to evaporation and condensation at both membrane walls, which affect the driving force and in turn has an effect on trans-membrane flux has been taken into account.

It is worthy to mention here that there are two different areas of the transport mechanism through the membrane pores (i.e., Knudsen diffusion and molecular diffusion), which affect the trans-membrane flux, in addition to the transport mechanism through the boundary layer of the osmotic agent (OA) side. Both these two transport mechanisms are useful for predicting the vapor transfer through the membrane and mainly depending on the pore radius of the membrane. In this case, molecular diffusion was the mode of diffusion when pore size is around 198.96 nm, and the values predicted by molecular diffusion are closely with the experimental data. It can be conclude that in the range of molecular diffusion

9

(large membrane pore size) the transmembrane flux is higher than that in the range of Knudsen diffusion. The transport mechanism through the boundary layer of the OA side is depend on the molar concentration of the osmotic agent (OA), activity coefficients of osmotic agent solutions at various concentrations and the saturation vapor pressure. The transmembrane flux is affected significantly by the osmotic agent concentration, as can be seen from Tables 2 and 3, and Fig. 3.

Conclusions

In this study, a thin Polytetrafluoroethylene (PTFE) macroporous layer supported by a polypropylene (PP) net (TF200 from pall–Gelman) (Flat-sheet membrane) was used in osmotic membrane distillation process. The influence of the osmotic agent concentration, such as $CaCl_2$ and NaCl solution on transmembrane flux was studied. The increase in the osmotic agent concentration in both cases resulted in an increase in transmembrane flux. The calcium chloride ($CaCl_2$) showed higher transmembrane flux as compared to sodium chloride (NaCl). The water fluxes were expressed as a function of the water activity difference between the solutions, which is the driving force of the process. Therefore, it was possible to compare the effect of the different osmotic agents. At high osmotic agent concentration, for example 4 and/or 5 mol/L, the transmembrane flux decreases as a function of time, due to the membrane fouling.

Classical gas and liquid mass transfer mechanisms were tested to simulate the performance of osmotic membrane distillation of pure water at 30 °C. The membrane mass transfer coefficient was described by molecular diffusion model and was estimated to be 1.196276E-02 kg m−2 h−1 Pa−1. It was observed that the mass transfer mechanism was in the molecular diffusion region when Knudsen number <0.01.

Based on the experimental results of the osmotic membrane distillation process for the pure water and osmotic agent solution separation, it is found that the model calculated values were 17% deviations with the experimental values.

Acknowledgments

Nomenclature

Symbol	Definition	Unit
C	Solute molar concentration	mol l−1
cp	Heat capacity	J kg−1 K−1
d	Diameter	m
D	Diffusion coefficient	m2 s−1
h	Heat transfer coefficient	W/m2.K
k	Mass transfer coefficient	m s−1
K	Mass transfer coefficient	kgm−2 h−1 Pa−1
KB	Boltzmann constant	1.3807*10−23 JK−1
kT	Thermal conductivity	Wm−1 K−1
L	Length of the fluid circulation channel	m
Mw	Molecular weight	kg mol−1
	Vapour flux, mass	kgm−2 h−1
J	Molar	molm−2 s−1
	or volume	m3 m−2 s−1
P	Pressure	Pa
P*	Saturation vapour pressure	Pa
Q	Heat flux	Wm−2
d	Pore diameter	m
R	Universal gas constant	8.314 JK−1 mol−1
T	Temperature	ºC. K
NA	Rotational speed of agitator	rps
x	mass fraction (w/w%) or molar fraction (mol/mol %)	
Yln	Mole fraction of air (log-mean)	

Greek symbols

ε	volume porosity factor	
δ	thickness	m
∆	difference	
γ	activity coefficient	

λ	mean molecular free path	m
μ	liquid dynamic viscosity	Pa s
χ	tortuosity factor	
ρ	liquid density	kgm^{-3}
σ	mean collision diameter	m
φ	association factor, 2.26 for water	
ν	Solute molar volume	m3 Kmol-1

Groups

Kn	Knudsen number
Nu	Nusselt number
Pr	Prandtl number
Re	Reynolds number
Sc	Schmidt number
Sh	Sherwood number

Subscripts

a	agitator
f	feed
h	hydraulic
L	liquid
Lm	logarithmic mean
m	membrane
p	permeate (brine)
s	solute
w	water or vapour

Superscripts

b	bulk location or exponent
K	Knudsen diffusion
m	membrane location
M	molecular diffusion
t	total

References

1. Lawson, K.W. and Lloyd, D.R., (1997), Membrane distillation. J. Membrane Sci., 124: 1–25.

2. Franken, A.C.M., Nolten, J.A.M., Mulder, M.H.V., Bargeman, D. and Smolders, C.A., (1987), Wetting criteria for the applicability of membrane distillation. J. Membrane Sci., 33: 285–298.

3. Hogan, P.A., Philip Canning, R., Peterson, P.A., Johnson, R.A. and Michaels, A.S., (1998), A new option: osmotic distillation. Chem .Eng. Prog., (July)

4. Mansouri, J. and Fane, A.G., (1999), Osmotic distillation of oily feeds. J. Membrane Sci., 153: 103–120.

5. Courel, M., Dornier, M., Rios, G.M. and Reynes, M., (2000), Modeling of water transport in osmotic distillation using asymmetric membrane. J. Membrane Sci., 173: 107-122.

6. Courel, M., Dornier, M., Herry, J.M., Rios, G.M. and Reynes, M., (2000), Effect of operating conditions on water transport during the concentration of sucrose solutions by osmotic distillation. J. Membrane Sci., 170: 281-289.

7. Nagaraj, N., Patil, Ganapathi, Ravindra Babu, B., Hebbar, U.H., Raghavarao, K.S.M.S. and Nene, S., (2006), Mass transfer in osmotic membrane distillation. J. Membrane Sci., 268: 48–56.

8. Ravindra Babu, B., Rastogi, N.K. and Raghavarao, K.S.M.S., (2006), Mass transfer in osmotic membrane distillation of phycocyanin colorant and sweet-lime juice. J. Membrane Sci., 272: 58–69.

9. Thanedgunbaworn, R., Jiraratananon, R. and Nguyen, M.H., (2007), Mass and heat transfer analysis in fructose concentration by osmotic distillation process using hollow fiber module. J .Food Eng., 78: 126–135.

10. Geankoplis, C.J., (1993), Principles of mass transfer. In Transport Processes and Unit Operations. (Prentice-Hall, London). pp. 381–413.

11. Datta, R., Dechapanichkul, S., Kim, J.S., Fang, L.Y. and Uehara, H., (1992), A generalized model for the transport of gases

in porous, non-porous, and leaky membranes I. Application to single gases. J. Membrane Sci., 75: 245–263.

12. Wilke, C.R. and Chang, P., (1955), Correlation of diffusion coefficients in dilute solutions. AIChE J., 1: 264.

13. Treybal, R.E., (1980). Mass Transfer Operations (3rd ed.). (McGraw Hill, New York).

14. Schofield, R.W., Fane, A.G. and Fell, C.J.D., (1987), Heat and mass transfer in membrane distillation. J. Membrane Sci., 33: 299.

15. Patil, K.R., Tripathi, A.D., Pathak, G. and Katti, S.S., (1991), Thermodynamic properties of aqueous electrolyte solutions. 2. Vapor pressure of aqueous solutions of NaBr, NaI, KCl, KBr, KI, RbCl, CsBr, MgCl2, CaCl2, CaBr2, CaI2, SrCl2, SrBr2, SrI2, BaCl2, and BaBr2. J. Chem. Eng. Data, 36: 225.

16. Colin, E., Clarke, W. and Glew, D.N., (1985), Evaluation of the thermodynamic functions for aqueous sodium chloride from equilibrium and calorimetric measurements below 154 °C. J. Phys Chem. Ref. Data, 14: 408.

17. Ananthaswamy, J. and Atkinson, G., (1985), Thermodynamics of concentrated electrolyte mixtures. 5. A review of the thermodynamic properties of aqueous calcium chloride in the temperature range 273.15–373.15 K. Chem. Eng. Data, 30: 120.

18. Kunz, Werner, Benhabiles, Ali and Ben-Kim, Roger., (1996), Osmotic evaporation through macroporous hydrophobic membranes: a survey of current research and applications. J. Membrane Sci., 121: 25–36.

19. Schofield, R.W., (1989), Membrane distillation, Ph.D. Thesis, University of New South Wales, Australia.

20. Speraty, C.A., (1989). Physical Constants of Fluoropolymers, Polymer Handbook (3rd ed.). (Wiley, New York).

21. Martinez-Diez, L., Florido-Diaz, F.J. and Vazquez- Gonzalez, M.I., (2000), Study of polarization phenomena in membrane distillation of aqueous salt solutions. Sep. Sci. Technol., 35:1485–1501.

22. Yun, Y., Ma, R., Zhang, W., Fane, A.G. and Li, J., (2006), Direct contact membrane distillation mechanism for high concentration NaCl solutions. Desalination, 188: 251–262.

23. Alves, V.D. and Coelhoso, I.M., (2004), Effect of membrane characteristics on mass and heat transfer in the osmotic evaporation process. J. Membrane Sci., 228: 159.

24. Gostoli, C., (1999), Thermal effects in osmotic distillation. J. Membrane Sci., 163: 75–91.

25. Perry, J.H., (1963). Chemical Engineers Handbook (4th ed.). (McGraw Hill, New York).